

PDF hosted at the Radboud Repository of the Radboud University Nijmegen

The following full text is a publisher's version.

For additional information about this publication click this link.

<http://hdl.handle.net/2066/50005>

Please be advised that this information was generated on 2017-12-11 and may be subject to change.

Acid-Base Status Determines the Renal Expression of Ca^{2+} and Mg^{2+} Transport Proteins

Tom Nijenhuis, Kirsten Y. Renkema, Joost G.J. Hoenderop, and René J.M. Bindels

Department of Physiology, Nijmegen Centre for Molecular Life Sciences, Radboud University Nijmegen Medical Centre, Nijmegen, The Netherlands

Chronic metabolic acidosis results in renal Ca^{2+} and Mg^{2+} wasting, whereas chronic metabolic alkalosis is known to exert the reverse effects. It was hypothesized that these adaptations are mediated at least in part by the renal Ca^{2+} and Mg^{2+} transport proteins. The aim of this study, therefore, was to determine the effect of systemic acid-base status on renal expression of the epithelial Ca^{2+} channel TRPV5, the Ca^{2+} -binding protein calbindin- $\text{D}_{28\text{K}}$, and the epithelial Mg^{2+} channel TRPM6 in relation to Ca^{2+} and Mg^{2+} excretion. Chronic metabolic acidosis that was induced by NH_4Cl loading or administration of the carbonic anhydrase inhibitor acetazolamide for 6 d enhanced calciuresis accompanied by decreased renal TRPV5 and calbindin- $\text{D}_{28\text{K}}$ mRNA and protein abundance in wild-type mice. In contrast, metabolic acidosis did not affect Ca^{2+} excretion in TRPV5 knockout (TRPV5 $^{-/-}$) mice, in which active Ca^{2+} reabsorption is effectively abolished. This demonstrates that downregulation of renal Ca^{2+} transport proteins is responsible for the hypercalciuria. Conversely, chronic metabolic alkalosis that was induced by NaHCO_3 administration for 6 d increased the expression of Ca^{2+} transport proteins accompanied by diminished urine Ca^{2+} excretion in wild-type mice. However, this Ca^{2+} -sparing action persisted in TRPV5 $^{-/-}$ mice, suggesting that additional mechanisms apart from upregulation of active Ca^{2+} transport contribute to the hypocalciuria. Furthermore, chronic metabolic acidosis decreased renal TRPM6 expression, increased Mg^{2+} excretion, and decreased serum Mg^{2+} concentration, whereas chronic metabolic alkalosis resulted in the exact opposite effects. In conclusion, these data suggest that regulation of Ca^{2+} and Mg^{2+} transport proteins contributes importantly to the effects of acid-base status on renal divalent handling.

J Am Soc Nephrol 17: 617–626, 2006. doi: 10.1681/ASN.2005070732

Acid-base homeostasis is known to affect renal handling of the divalents Ca^{2+} and Mg^{2+} (1–3). Chronic metabolic acidosis, which can occur as a result of clinical disorders such as renal failure, distal renal tubular acidosis, or chronic diarrhea, is associated with increased renal Ca^{2+} and Mg^{2+} excretion. Long-standing metabolic acidosis can lead to Ca^{2+} loss from bone and ultimately results in metabolic bone disease, including osteomalacia and osteoporosis (4). Conversely, chronic metabolic alkalosis in, for example, the milk-alkali syndrome, volume contraction, or treatment of nephrolithiasis by bicarbonate supplementation is known to decrease urine Ca^{2+} and Mg^{2+} excretion (1,3). However, the molecular mechanisms that explain the altered renal divalent excretion during these disturbances of acid-base balance remain unknown.

The major part of Ca^{2+} and Mg^{2+} reabsorption takes place in the proximal tubule and thick ascending limb of the loop of Henle (TAL) through a passive paracellular pathway (1,3). Fine-tuning of divalent excretion by the kidney occurs in the distal convoluted tubule (DCT) and the connecting tubule

(CNT). In the latter segments, active transcellular Ca^{2+} and Mg^{2+} reabsorption determines the final amount excreted into the urine. Active Ca^{2+} reabsorption consists of Ca^{2+} entry through the apically localized epithelial Ca^{2+} channel TRPV5, cytosolic transport bound to the calcium-binding and buffering protein calbindin- $\text{D}_{28\text{K}}$, and basolateral extrusion by the Na^+ / Ca^{2+} exchanger (NCX1) and a plasma membrane Ca^{2+} ATPase (PMCA1b) (1,5,6). Studying the regulation of active Mg^{2+} reabsorption in DCT has been seriously hampered by the lack of identification of the proteins involved (3). TRPM6 was recently identified as a Mg^{2+} permeable channel predominantly expressed along the apical membrane of DCT (7). Mutations in TRPM6 cause autosomal recessive hypomagnesemia, characterized by inappropriately high fractional Mg^{2+} excretion rates and disturbed intestinal Mg^{2+} absorption (8,9). This clearly suggests that TRPM6 constitutes the apical entry step in active Mg^{2+} (re)absorption and thus provides an important new tool to study this process at the molecular level (7).

Earlier studies, including micropuncture experiments, suggested that systemic acid-base disturbances specifically influence Ca^{2+} and Mg^{2+} reabsorption in DCT/CNT (2,10). Hypothetically, regulation of Ca^{2+} and Mg^{2+} transport proteins in these nephron segments could be involved in the altered renal divalent excretion secondary to changes in acid-base status, as was shown for other renal transporters and channels (11–14). We previously demonstrated that tacrolimus (FK506)-induced Ca^{2+} and Mg^{2+} wasting as well as thiazide-induced hypomag-

Received July 15, 2005. Accepted December 5, 2005.

Published online ahead of print. Publication date available at www.jasn.org.

Address correspondence to: Dr. René J.M. Bindels, 286 Cell Physiology, Radboud University Nijmegen Medical Centre, PO Box 9101, NL-6500 HB Nijmegen, The Netherlands. Phone: +31-24-3614211; Fax: +31-24-3616413; E-mail: r.bindels@ncmls.ru.nl

nesemia are associated with decreased renal expression of Ca^{2+} and/or Mg^{2+} transporters (15,16). Recently, TRPV5 knockout ($\text{TRPV5}^{-/-}$) mice were generated in our laboratory, which display a robust renal Ca^{2+} leak localized to DCT/CNT, illustrating that active Ca^{2+} reabsorption is effectively abolished (17). These mice constitute a unique mouse model to determine the role of TRPV5 and active Ca^{2+} reabsorption in acid-base induced alterations of calciuresis.

The aim of this study, therefore, was to determine the effect of chronic metabolic acidosis and alkalosis on the expression of Ca^{2+} and Mg^{2+} transporters in the kidney and to evaluate their contribution to the altered Ca^{2+} and Mg^{2+} excretion. We induced metabolic alkalosis by oral NaHCO_3 loading and metabolic acidosis by NH_4Cl loading, as well as applied acetazolamide administration in wild-type and $\text{TRPV5}^{-/-}$ mice. Acetazolamide specifically inhibits proximal tubular HCO_3^- reabsorption, resulting in a self-limiting metabolic acidosis with, in contrast to NH_4Cl loading, an alkaline urine pH (18–20). This enabled evaluation of the role of luminal pH. Furthermore, whereas acidosis generally increases urine Mg^{2+} excretion, acetazolamide is known for its unexplained Mg^{2+} -sparing action (21–23).

Materials and Methods

Metabolic Acidosis and Alkalosis in Wild-Type and $\text{TRPV5}^{-/-}$ Mice

Metabolic Acidosis. $\text{TRPV5}^{-/-}$ mice were recently generated by targeted ablation of the TRPV5 gene and genotyped as described previously (17). Ten-week-old wild-type ($\text{TRPV5}^{+/+}$) mice and $\text{TRPV5}^{-/-}$ littermates were kept in a light- and temperature-controlled room with *ad libitum* access to deionized drinking water. Mice were ration-fed standard pelleted chow (0.25% [wt/wt] NaCl, 1.1% [wt/wt] Ca, 0.2% [wt/wt] Mg) during the metabolic balance studies. For evaluation of the effects of metabolic acidosis, mice were randomly assigned to a group that received either 0.28 M ($\text{TRPV5}^{+/+}$) or 0.14 M ($\text{TRPV5}^{-/-}$) NH_4Cl *via* the drinking water during 6 d or a control group that received normal deionized drinking water. NH_4Cl loading is a generally accepted and validated method to induce metabolic acidosis in rodents (11–13,24). Because the oral fluid intake of $\text{TRPV5}^{-/-}$ mice is approximately two-fold higher than that in wild-type mice, the lower NH_4Cl concentration in their drinking water ensured a similar oral acid load compared with wild-type mice to prevent acid overloading in these $\text{TRPV5}^{-/-}$ mice. Alternatively, subcutaneous administration of the carbonic anhydrase inhibitor acetazolamide (20 mg/kg per d) during 6 d by osmotic minipumps was applied. This enabled evaluation of the role of urine pH in metabolic acidosis-induced changes in Ca^{2+} excretion as well as the role of TRPM6 in the unexplained Mg^{2+} -sparing action of acetazolamide.

Metabolic Alkalosis. Metabolic alkalosis was induced by oral administration of 0.2 and 0.1 M NaHCO_3 to $\text{TRPV5}^{+/+}$ and $\text{TRPV5}^{-/-}$ mice, respectively. NaHCO_3 loading was previously shown to induce metabolic alkalosis in rodents (12,13). Mice that received 0.2 or 0.1 M NaCl constituted the control group, thereby correcting for possible effects of the increased Na^+ load. The latter is particularly important because passive Ca^{2+} reabsorption is functionally coupled to Na^+ reabsorption. Mice were treated for 6 d, after which they were housed in metabolic cages to enable collection of 24-h urine samples under mineral oil, preventing evaporation. At the end of the experiment, the mice were killed, blood samples were taken, and kidneys were sam-

pled. The animal ethics board of the Radboud University Nijmegen approved all animal studies.

Analytical Procedures

Serum and urine Ca^{2+} and Mg^{2+} concentrations were determined using colorimetric assays as described previously (16,25). Blood gas measurements were performed using a Hitachi auto-analyzer (Hitachi, Laval, Quebec, Canada). Na^+ , K^+ , and Li^+ concentrations were measured flame-spectrophotometrically (Eppendorf FCM 6343, Hamburg, Germany). Urine pH was determined using an electronic ion analyzer (Hanna Instruments, Szeged, Hungary), and osmolarity was measured with an Osmette A automatic osmometer (Precision Instruments, Sudbury, MA).

Real-Time Quantitative PCR

Total RNA was extracted from kidney using TriZol Total RNA Isolation Reagent (Life Technologies BRL, Breda, The Netherlands). The obtained RNA was subjected to DNase treatment and reverse transcribed using Molony-Murine Leukemia Virus-Reverse Transcriptase (Life Technologies BRL) as described previously (26,27). Subsequently, the acquired cDNA was used to determine TRPV5, calbindin- $\text{D}_{28\text{K}}$, and TRPM6 mRNA levels in kidney by real-time quantitative PCR on an ABI Prism 7700 Sequence Detection System (PE Biosystems, Rotkreuz, Switzerland) as described previously (15,26). In addition, mRNA expression of the housekeeping gene hypoxanthine-guanine phosphoribosyl transferase was determined as an endogenous control, which enabled calculation of specific mRNA expression levels as a ratio of hypoxanthine-guanine phosphoribosyl transferase.

Immunohistochemistry

Staining of kidney sections for TRPV5, calbindin- $\text{D}_{28\text{K}}$, and TRPM6 was performed on cryosections of periodate-lysine-paraformaldehyde-fixed kidney samples as described previously (7,28). For semiquantitative determination of protein abundance, images were made using a Zeiss fluorescence microscope equipped with a digital camera (Nikon DXM1200), which were analyzed with the Image Pro Plus 4.1 image analysis software (Media Cybernetics, Silver Spring, MD). The entire cortex in two separate kidney sections of each animal was included in the analysis, resulting in quantification of protein levels as the mean of integrated optical density.

Immunoblotting

Calbindin- $\text{D}_{28\text{K}}$ protein levels were semiquantified by immunoblotting as described previously (27). In short, kidney cortex sections were homogenized and samples were normalized according to protein concentration. Subsequently, protein samples were separated on 16.5% (wt/vol) SDS-PAGE gels and blotted to polyvinylidene difluoride-nitrocellulose membranes (Immunobilon-P; Millipore Corp., Bedford, MA), and protein was detected using a rabbit calbindin- $\text{D}_{28\text{K}}$ antibody.

Statistical Analyses

Data are expressed as means \pm SEM. Statistical comparisons were analyzed by one-way ANOVA and Fisher multiple comparison. $P < 0.05$ was considered statistically significant. All analyses were performed using the StatView Statistical Package software (Power PC version 4.51, Berkely, CA) on an Apple iMac computer.

Results

Metabolic Acidosis and Alkalosis in Wild-Type and $\text{TRPV5}^{-/-}$ Mice

Oral NH_4Cl loading induced a similar metabolic acidosis in wild-type and $\text{TRPV5}^{-/-}$ mice, as demonstrated by the signif-

Table 1. Acid-base status during different treatment protocols in TRPV5^{+/+} and TRPV5^{-/-} mice^a

	TRPV5 ^{+/+}		TRPV5 ^{-/-}	
	pH	[HCO ₃ ⁻] (mM)	pH	[HCO ₃ ⁻] (mM)
Controls	7.27 ± 0.01	22.3 ± 0.7	7.26 ± 0.03	21.0 ± 0.5
NH ₄ Cl	7.11 ± 0.05 ^b	17.2 ± 1.3 ^b	7.16 ± 0.01 ^b	18.3 ± 0.7 ^b
ACTZ	7.22 ± 0.02 ^b	19.0 ± 0.9 ^b	7.22 ± 0.01	23.1 ± 0.9
NaCl	7.27 ± 0.02	22.6 ± 0.8	7.25 ± 0.02	21.7 ± 0.5
NaHCO ₃	7.35 ± 0.01 ^{b,c}	25.8 ± 1.0 ^{b,c}	7.35 ± 0.01 ^{b,c}	36.3 ± 3.8 ^{b,c}

^aControls, animals that received deionized drinking water only; NH₄Cl, animals that received 0.28 (TRPV5^{+/+}) or 0.14 M (TRPV5^{-/-}) NH₄Cl *via* the drinking water; ACTZ, animals that received acetazolamide (20 mg/kg per d) subcutaneously by osmotic minipump; NaCl, animals that received 0.2 (TRPV5^{+/+}) or 0.1 M (TRPV5^{-/-}) NaCl *via* the drinking water; NaHCO₃, animals that received 0.2 (TRPV5^{+/+}) or 0.1 M (TRPV5^{-/-}) NaHCO₃ *via* the drinking water. Data are presented as means ± SEM.

^b*P* < 0.05 *versus* respective TRPV5^{+/+} or TRPV5^{-/-} controls.

^c*P* < 0.05 *versus* respective TRPV5^{+/+} or TRPV5^{-/-} NaCl-treated mice.

icantly reduced blood pH and HCO₃⁻ concentration (Table 1). Accordingly, NH₄Cl reduced urine pH in wild-type and TRPV5^{-/-} mice compared with their respective controls (Table 2). Likewise, chronic acetazolamide treatment significantly increased urine pH and decreased blood pH and HCO₃⁻ concentration in wild-type but not in TRPV5^{-/-} mice. Of note, acetazolamide-induced acidosis and urinary alkalization is often self-limiting. Indeed, urine pH was more alkaline in all animals after 3 d compared with day 6 of treatment (data not shown). Furthermore, blood gas determination substantiated the effectiveness of the oral NaHCO₃ loading protocol in wild-type and TRPV5^{-/-} mice. Serum pH was similar in both genotypes

during NaHCO₃ loading, whereas serum HCO₃⁻ levels in TRPV5^{-/-} mice were significantly higher. This reflects higher pCO₂ in the latter situation, most probably as a result of differences in time or depth of anesthesia. The absence of this difference in pCO₂ between wild-type and TRPV5^{-/-} mice in the other treatment groups suggests that there is no intrinsic increased susceptibility to retain CO₂ in TRPV5^{-/-} mice. It is interesting that urine pH was consistently 0.5 to 1 pH unit lower in TRPV5^{-/-} mice as compared with the corresponding wild-type mice, but, importantly, TRPV5^{-/-} mice did not display metabolic acidosis at baseline. Diuresis and Na⁺ excretion were not affected by NH₄Cl or NaHCO₃ loading, whereas

Table 2. Urine composition and fluid intake during chronic metabolic acidosis and alkalosis in TRPV5^{+/+} and TRPV5^{-/-} mice^a

	pH	Urine Volume (mL/24 h)	Na ⁺ Excretion (mmol/24 h)	K ⁺ Excretion (mmol/24 h)	Li ⁺ Clearance (μL/min)	Urine Osmolarity (mOsmol/kg)	Fluid Intake (mL/24 h)
TRPV5 ^{+/+}							
controls	7.0 ± 0.2	5.3 ± 1.4	0.4 ± 0.1	1.4 ± 0.1	13 ± 1	2434 ± 175	16.9 ± 3.8
NH ₄ Cl	6.0 ± 0.1 ^b	5.1 ± 0.7	0.5 ± 0.1	1.2 ± 0.1	11 ± 1	2710 ± 246	12.1 ± 0.3
ACTZ	8.3 ± 0.1 ^b	9.7 ± 0.9 ^b	0.7 ± 0.2 ^b	1.9 ± 0.3 ^b	19 ± 3 ^b	1720 ± 64 ^b	20.4 ± 2.5
NaCl	7.5 ± 0.2	17.1 ± 1.7 ^b	3.6 ± 0.3 ^b	1.4 ± 0.1	30 ± 2 ^b	1484 ± 52 ^b	26.7 ± 4.8
NaHCO ₃	8.8 ± 0.1 ^{b,c}	10.8 ± 3.3 ^b	1.6 ± 0.2 ^{b,c}	1.0 ± 0.1 ^c	17 ± 3 ^{b,c}	1540 ± 146 ^b	27.4 ± 2.4
TRPV5 ^{-/-}							
controls	6.0 ± 0.1	18.7 ± 2.4	0.5 ± 0.1	1.5 ± 0.1	16 ± 2	1113 ± 101	30.6 ± 3.3
NH ₄ Cl	5.4 ± 0.1 ^b	15.8 ± 1.7	0.5 ± 0.1	1.3 ± 0.2	13 ± 2	1488 ± 99	26.4 ± 4.1
ACTZ	7.4 ± 0.2 ^b	33.1 ± 4.0 ^b	0.9 ± 0.1 ^b	2.3 ± 0.1 ^b	19 ± 1 ^b	709 ± 28 ^b	44.6 ± 4.8
NaCl	6.1 ± 0.1	23.6 ± 2.2 ^b	3.1 ± 0.5 ^b	1.4 ± 0.1	25 ± 2 ^b	1000 ± 30	29.4 ± 7.5
NaHCO ₃	8.3 ± 0.1 ^{b,c}	18.6 ± 5.7	1.3 ± 0.1 ^{b,c}	0.6 ± 0.1 ^{b,c}	11 ± 2 ^{b,c}	1036 ± 90	37.1 ± 1.1

^aControls, animals that received deionized drinking water only; NH₄Cl, animals that received 0.28 (TRPV5^{+/+}) or 0.14 M (TRPV5^{-/-}) NH₄Cl *via* the drinking water; ACTZ, animals that received acetazolamide (20 mg/kg per d) subcutaneously by osmotic minipump; NaCl, animals that received 0.2 (TRPV5^{+/+}) or 0.1 M (TRPV5^{-/-}) NaCl *via* the drinking water; NaHCO₃, animals that received 0.2 (TRPV5^{+/+}) or 0.1 M (TRPV5^{-/-}) NaHCO₃ *via* the drinking water; *n* = 9 animals per treatment group; *n* = 3 animals per cage. Data are presented as means ± SEM.

^b*P* < 0.05 *versus* respective TRPV5^{+/+} or TRPV5^{-/-} controls.

^c*P* < 0.05 *versus* respective TRPV5^{+/+} or TRPV5^{-/-} NaCl-treated mice.

acetazolamide significantly increased urine volume and natriuresis in wild-type and TRPV5^{-/-} mice (Table 2).

Ca²⁺ Homeostasis during Chronic Metabolic Acidosis and Alkalosis

Genetic ablation of TRPV5 resulted in a strikingly increased calciuresis compared with wild-type littermates (Figure 1A). NH₄Cl loading significantly enhanced urine Ca²⁺ excretion in wild-type mice, whereas Ca²⁺ excretion was not affected in TRPV5^{-/-} mice. Likewise, acetazolamide treatment significantly enhanced calciuresis in wild-type mice, whereas this effect was not present in TRPV5^{-/-} mice. Serum Ca²⁺ levels remained unaltered during NH₄Cl loading and acetazolamide treatment (Figure 1C). In contrast to metabolic acidosis, NaHCO₃ administration significantly reduced urine Ca²⁺ ex-

cretion in wild-type as well as in TRPV5^{-/-} mice (Figure 1B). Serum Ca²⁺ levels and urine volume did not differ between the alkalosis and control groups (Figure 1D, Table 1). Because Li⁺ and Na⁺ are transported in parallel by the proximal tubule, endogenous Li⁺ clearance was used as an inverse measure of proximal tubular Na⁺ reabsorption, to which in turn passive Ca²⁺ reabsorption is functionally coupled (16). Li⁺ clearance was significantly increased by acetazolamide treatment and NaCl loading in wild-type and TRPV5^{-/-} mice, suggesting decreased proximal tubular Na⁺ reabsorption (Table 1). Conversely, NaHCO₃ loading decreased Li⁺ clearance compared with NaCl-treated controls.

Mg²⁺ Homeostasis during Chronic Metabolic Acidosis and Alkalosis

In addition, we evaluated the effect of the different treatment protocols on renal Mg²⁺ homeostasis in wild-type mice. Oral NH₄Cl loading significantly enhanced Mg²⁺ excretion (Figure 2A), which was accompanied by decreased serum Mg²⁺ levels (Figure 2C). In contrast, acetazolamide displayed a Mg²⁺-sparing effect accompanied by a significantly increased serum Mg²⁺ concentration. Likewise, metabolic alkalosis that was induced by NaHCO₃ treatment significantly reduced urine Mg²⁺ excretion (Figure 2B) and increased the serum Mg²⁺ level (Figure 2D).

Renal mRNA and Protein Expression of Ca²⁺ Transporters

For studying the effect of systemic acid-base status on renal Ca²⁺ transporter expression, TRPV5 and calbindin-D_{28K} mRNA levels were determined by real-time quantitative PCR analysis, and protein abundance was analyzed by immunohistochemistry and immunoblotting. NH₄Cl loading significantly reduced both TRPV5 and calbindin-D_{28K} mRNA levels in kidney cortex of wild-type mice (Figure 3, A and C). Calbindin-D_{28K} mRNA levels were significantly decreased in TRPV5^{-/-} compared with TRPV5^{+/+} mice. In addition, NH₄Cl treatment further reduced calbindin-D_{28K} mRNA levels compared with control TRPV5^{-/-} mice. Figure 4A shows representative immunohistochemical images of kidney cortex probed with anti-TRPV5 and anti-calbindin-D_{28K} antibodies. In addition, calbindin-D_{28K} protein abundance was determined by immunoblotting (Figure 4B). In line with the mRNA levels, semi-quantification of the immunohistochemical analysis showed that NH₄Cl decreases TRPV5 and calbindin-D_{28K} protein abundance (Figure 5, A and C). These results were confirmed by immunoblotting (100 ± 4 versus 63 ± 9% in wild-type and 100 ± 5 versus 75 ± 8% in TRPV5^{-/-} mice, respectively). Acetazolamide treatment decreased TRPV5 mRNA and protein expression in wild-type mice (Figures 3A and 5A). Furthermore, calbindin-D_{28K} protein abundance was reduced in acetazolamide-treated mice (Figure 5C), as confirmed by immunoblotting (100 ± 1 versus 63 ± 6 and 40 ± 8% in wild-type and TRPV5^{-/-} mice, respectively). In contrast to metabolic acidosis, chronic metabolic alkalosis that was induced by NaHCO₃ loading increased TRPV5 mRNA and protein expression in wild-type mice (Figures 3B and 5B). Likewise, calbindin-D_{28K} expression was increased as determined by real-time PCR and immunohistochemistry (Figures 3D and 5D), as well as by

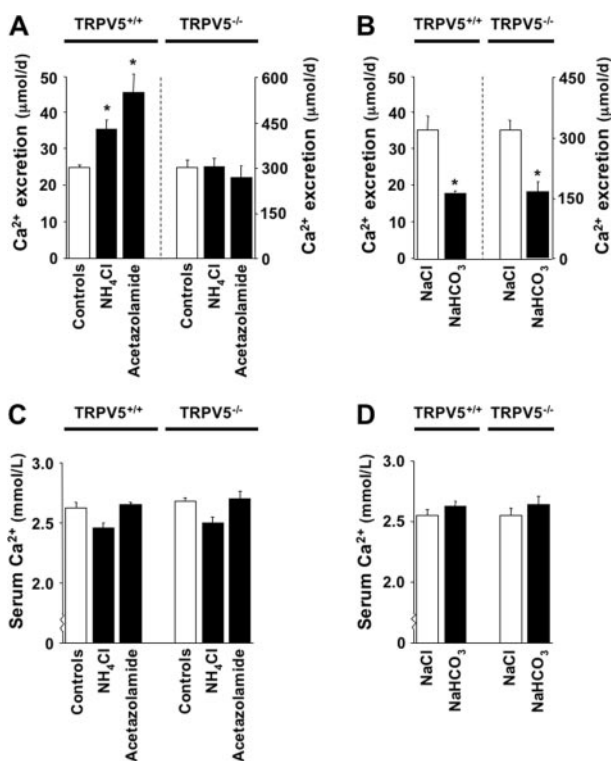


Figure 1. Urinary Ca²⁺ excretion and serum Ca²⁺ concentration during metabolic acidosis and alkalosis in wild-type (TRPV5^{+/+}) and TRPV5 knockout (TRPV5^{-/-}) mice. The effects of chronic metabolic acidosis and acetazolamide (A) as well as during metabolic alkalosis (B) on renal Ca²⁺ excretion and serum Ca²⁺ concentration (C and D) were determined in metabolic cage experiments (*n* = 9 animals; *n* = 3 animals per cage). Controls, animals that received deionized drinking water only; NH₄Cl, animals that received 0.28 M (TRPV5^{+/+}) or 0.14 M (TRPV5^{-/-}) NH₄Cl *via* the drinking water; Acetazolamide, animals that received acetazolamide (20 mg/kg per d) subcutaneously by osmotic minipump; NaCl, animals that received 0.2 (TRPV5^{+/+}) or 0.1 M (TRPV5^{-/-}) NaCl *via* the drinking water; NaHCO₃, animals that received 0.2 (TRPV5^{+/+}) or 0.1 M (TRPV5^{-/-}) NaHCO₃ *via* the drinking water. Data are presented as means ± SEM. **P* < 0.05 *versus* respective TRPV5^{+/+} or TRPV5^{-/-} control group (controls or NaCl-treated animals).

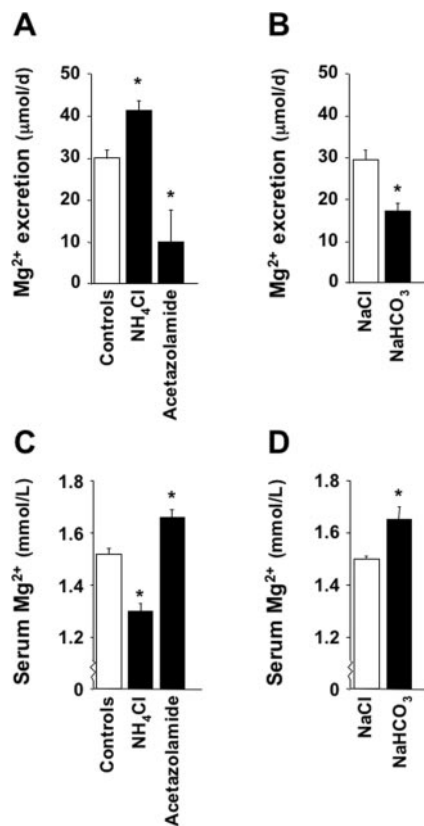


Figure 2. Urinary Mg²⁺ excretion and serum Mg²⁺ concentration during metabolic acidosis and alkalosis in wild-type mice. The effects of chronic metabolic acidosis and acetazolamide (A) as well as during metabolic alkalosis (B) on renal Mg²⁺ excretion and serum Mg²⁺ concentration (C and D) were determined in metabolic cage experiments ($n = 9$ animals; $n = 3$ animals per cage). Controls, animals that received deionized drinking water only; NH₄Cl, animals that received 0.28 M NH₄Cl *via* the drinking water; Acetazolamide, animals that received acetazolamide (20 mg/kg per d) subcutaneously by osmotic minipump; NaCl, animals that received 0.2 M NaCl *via* the drinking water; NaHCO₃, animals that received 0.2 M NaHCO₃ *via* the drinking water. Data are presented as means \pm SEM. * $P < 0.05$ versus respective control group (controls or NaCl-treated animals).

immunoblotting (100 ± 41 versus $293 \pm 40\%$). Conversely, calbindin-D_{28K} mRNA and protein levels were not significantly increased in NaHCO₃-treated TRPV5^{-/-} mice.

Effect of Acid-Base Status on Renal TRPM6 Expression

Renal TRPM6 mRNA and protein expression levels were determined by real-time quantitative PCR analysis (Figure 6) and semi-quantitative immunohistochemistry (Figure 7A). Both NH₄Cl loading and acetazolamide treatment significantly reduced renal TRPM6 mRNA as well as protein abundance in wild-type mice (Figures 6A and 7B), whereas NaHCO₃-treated mice displayed increased TRPM6 expression (Figures 6B and 7C).

Discussion

This study demonstrated that systemic acid-base status regulates the expression of proteins that are involved in active

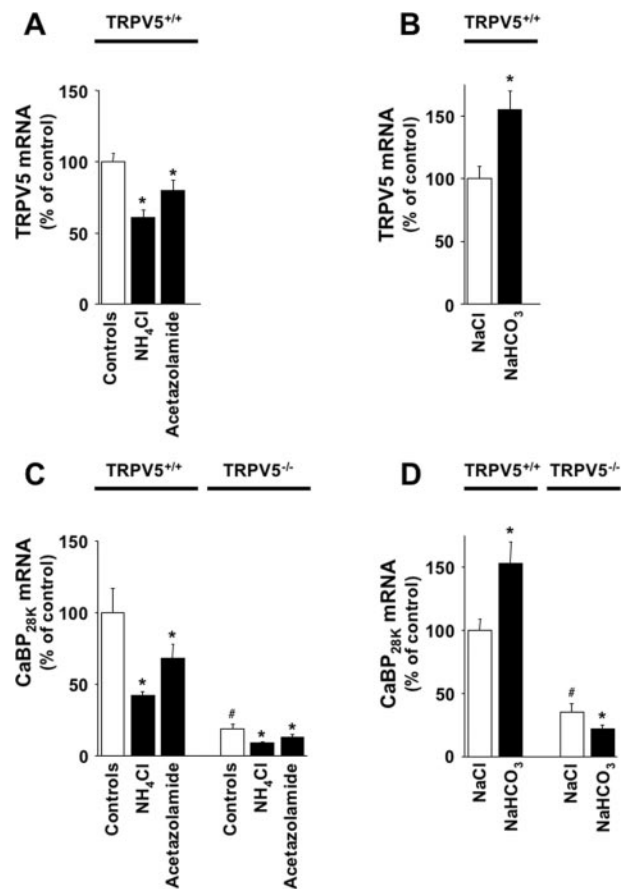


Figure 3. Effect of chronic metabolic acidosis and alkalosis on renal mRNA expression of Ca²⁺ transport proteins in TRPV5^{+/+} and TRPV5^{-/-} mice. Renal mRNA expression levels of the epithelial Ca²⁺ channel TRPV5 and the cytosolic Ca²⁺-binding protein calbindin-D_{28K} (CaBP_{28K}) were determined during chronic metabolic acidosis and acetazolamide treatment (A and C, respectively) and chronic metabolic alkalosis (B and D, respectively) by real-time quantitative PCR analysis as the ratio of hypoxanthine-guanine phosphoribosyl transferase (HPRT) and depicted as percentage of respective controls. Controls, animals that received deionized drinking water only; NH₄Cl, animals that received 0.28 (TRPV5^{+/+}) or 0.14 M (TRPV5^{-/-}) NH₄Cl *via* the drinking water; Acetazolamide, animals that received acetazolamide (20 mg/kg per d) subcutaneously by osmotic minipump; NaCl, animals that received 0.2 (TRPV5^{+/+}) or 0.1 M (TRPV5^{-/-}) NaCl *via* the drinking water; NaHCO₃, animals that received 0.2 (TRPV5^{+/+}) or 0.1 M (TRPV5^{-/-}) NaHCO₃ *via* the drinking water; $n = 9$ animals per group. Data are presented as means \pm SEM. * $P < 0.05$ versus respective TRPV5^{+/+} or TRPV5^{-/-} control group (controls or NaCl-treated animals); # $P < 0.05$ versus TRPV5^{+/+} controls.

Ca²⁺ and Mg²⁺ reabsorption. Our data showed that downregulation of renal Ca²⁺ transport proteins is responsible for the hypercalciuria during chronic metabolic acidosis. In contrast, the Ca²⁺-sparing effect of chronic metabolic alkalosis was associated with enhanced Ca²⁺ transporter abundance. However, the Ca²⁺-sparing action persisted in TRPV5^{-/-} mice, suggesting that additional mechanisms apart from upregulation of active Ca²⁺ transport contribute to the hypocalciuria. Further-

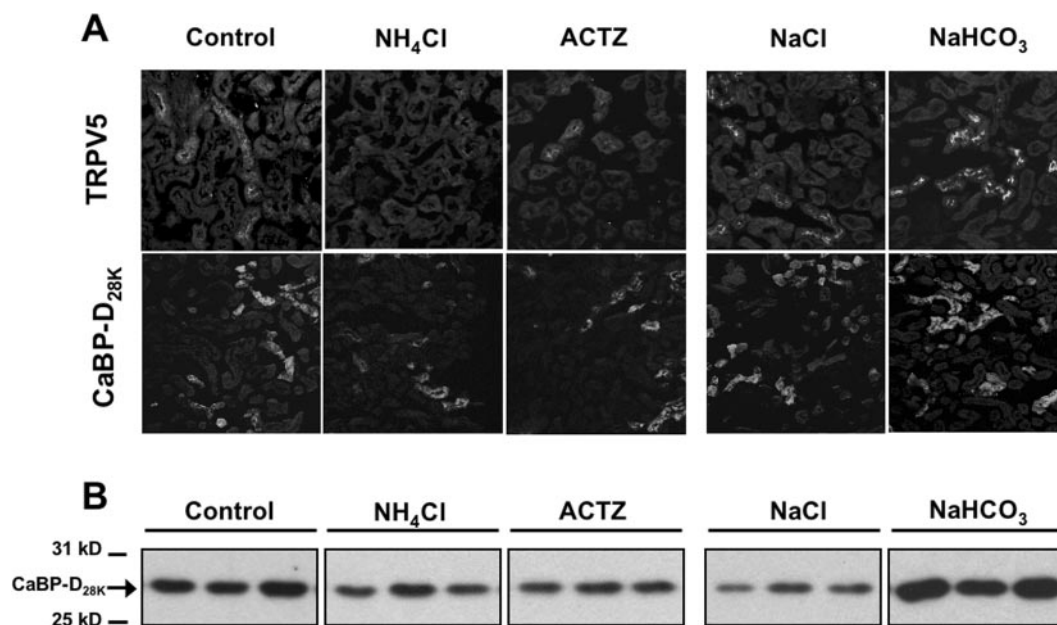


Figure 4. Immunohistochemical staining and semiquantitative immunoblotting of renal Ca^{2+} transport proteins in $\text{TRPV5}^{+/+}$ mice. (A) Representative immunohistochemical images of TRPV5 and $\text{CaBP}_{28\text{K}}$ staining in kidney cortex of wild-type mice. (B) Representative immunoblots for calbindin- $\text{D}_{28\text{K}}$. Controls, animals that received deionized drinking water only; NH_4Cl , animals that received 0.28 M NH_4Cl *via* the drinking water; ACTZ, animals that received acetazolamide (20 mg/kg per d) subcutaneously by osmotic minipump; NaCl, animals that received 0.2 M NaCl *via* the drinking water; NaHCO_3 , animals that received 0.2 M NaHCO_3 *via* the drinking water.

more, metabolic acidosis decreased renal TRPM6 abundance as well as Mg^{2+} reabsorption, whereas metabolic alkalosis had the opposite effect. These data indicate that regulation of TRPM6 explains the effects of acid-base status on renal Mg^{2+} handling.

Chronic metabolic acidosis that was induced by NH_4Cl loading enhanced Ca^{2+} excretion and decreased the expression of the epithelial Ca^{2+} channel TRPV5 and the cytosolic Ca^{2+} -binding and buffering protein calbindin- $\text{D}_{28\text{K}}$ in wild-type mice. Both proteins play a central role in active Ca^{2+} reabsorption in DCT/CNT (1). We showed that 0.14 M NH_4Cl loading induced a similar metabolic acidosis in polydipsic $\text{TRPV5}^{-/-}$ mice compared with wild-type mice. Importantly, Ca^{2+} excretion was not altered during chronic metabolic acidosis in $\text{TRPV5}^{-/-}$ mice, in which active Ca^{2+} reabsorption is effectively abolished (17). These results indicated that downregulation of Ca^{2+} transport proteins that are present in DCT/CNT underlies the increased Ca^{2+} excretion during NH_4Cl loading. Alternatively, increased Ca^{2+} mobilization from bone has been shown in chronic metabolic acidosis and was suggested to explain the Ca^{2+} wasting (4,29). Our study provides evidence for a primary renal Ca^{2+} leak. In line with our data, previous micropuncture experiments suggested that tubular Ca^{2+} reabsorption in DCT/CNT is specifically diminished during chronic metabolic acidosis in dogs (2). In contrast, Rizzo *et al.* (30) previously reported that NH_4Cl -induced acidosis in rats was accompanied by a moderate although significant increase of calbindin- $\text{D}_{28\text{K}}$. The reason for the discrepancy with our study, which shows a consistent decrease of TRPV5 and calbindin- $\text{D}_{28\text{K}}$ mRNA as well as protein expression, is not known.

Mice that receive NH_4Cl develop chronic metabolic acidosis that is characterized by a slight decrease in blood pH, a reduced serum HCO_3^- concentration, and, importantly, a low urine pH as substantiated in this study (24). Vennekens *et al.* (31) recently demonstrated that extracellular protons inhibit TRPV5 *in vitro* by titrating glutamate 522 in the extracellular loop between the fifth putative transmembrane domain and the pore region as shown by Yeh *et al.* (32). Therefore, it was suggested that acidification of the DCT/CNT luminal fluid during chronic metabolic acidosis explains the decreased Ca^{2+} reabsorption *in vivo* (31,32). These data raised the question of whether the regulation of Ca^{2+} transport proteins is secondary to the acidosis *per se* or due to the low urine pH. This urine acidification has been attributed mainly to parallel enhancement of apical Na^+/H^+ exchanger (NHE3) and basolateral $\text{Na}^+-\text{HCO}_3^-$ co-transporter activity in the proximal tubule (33–36). In contrast, acetazolamide treatment is known to induce metabolic acidosis by diminishing this proximal tubular HCO_3^- reabsorptive capacity (18–20). This would result in an increased luminal pH at more distal nephron segments, including TRPV5 and calbindin- $\text{D}_{28\text{K}}$ -expressing DCT/CNT. In our study, acetazolamide-treated mice indeed displayed urine alkalinization. Importantly, acetazolamide downregulated the expression of Ca^{2+} transport proteins. Thus, luminal pH in DCT/CNT does not seem to be crucial in the long-term *in vivo* hypercalciuric effect of chronic metabolic acidosis. Therefore, our data provide a molecular explanation for the increased Ca^{2+} excretion in clinically relevant situations, including chronic renal failure, chronic diarrhea, and renal tubular acidosis. In particular, acetazolamide treatment is a common cause of proximal renal tubular acidosis and is

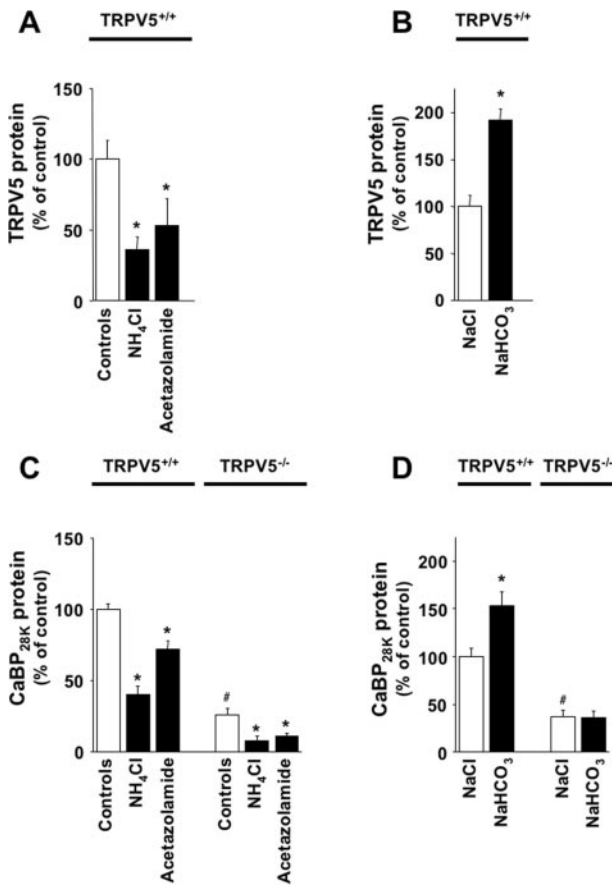


Figure 5. Effect of chronic metabolic acidosis and alkalosis on renal protein abundance of Ca²⁺ transport proteins in TRPV5^{+/+} and TRPV5^{-/-} mice. Renal protein expression levels of the epithelial Ca²⁺ channel TRPV5 and the cytosolic CaBP_{28K} were determined during chronic metabolic acidosis and acetazolamide treatment (A and C, respectively) as well as chronic metabolic alkalosis (B and D, respectively) by computerized analysis of immunohistochemical images. Data were calculated as integrated optical density (IOD; arbitrary units) and depicted as percentage of respective controls. Controls, animals that received deionized drinking water only; NH₄Cl, animals that received 0.28 (TRPV5^{+/+}) or 0.14 M (TRPV5^{-/-}) NH₄Cl *via* the drinking water; Acetazolamide, animals that received acetazolamide (20 mg/kg per d) subcutaneously by osmotic minipump; NaCl, animals that received 0.2 (TRPV5^{+/+}) or 0.1 M (TRPV5^{-/-}) NaCl *via* the drinking water; NaHCO₃, animals that received 0.2 (TRPV5^{+/+}) or 0.1 M (TRPV5^{-/-}) NaHCO₃ *via* the drinking water; *n* = 9 animals per treatment group. Data are presented as means ± SEM. **P* < 0.05 *versus* respective TRPV5^{+/+} or TRPV5^{-/-} control group (controls or NaCl-treated animals); #*P* < 0.05 *versus* TRPV5^{+/+} controls.

often associated with Ca²⁺ nephrolithiasis (37,38). Taken together, we showed that systemic metabolic acidosis, as opposed to associated changes in urine pH, downregulates Ca²⁺ transport proteins and, thereby, induces hypercalciuria.

Conversely, chronic metabolic alkalosis is known to decrease Ca²⁺ excretion (2). In this study, chronic NaHCO₃ administration induced metabolic alkalosis in wild-type as well as TRPV5^{-/-} mice. Chronic metabolic alkalosis had a Ca²⁺-spar-

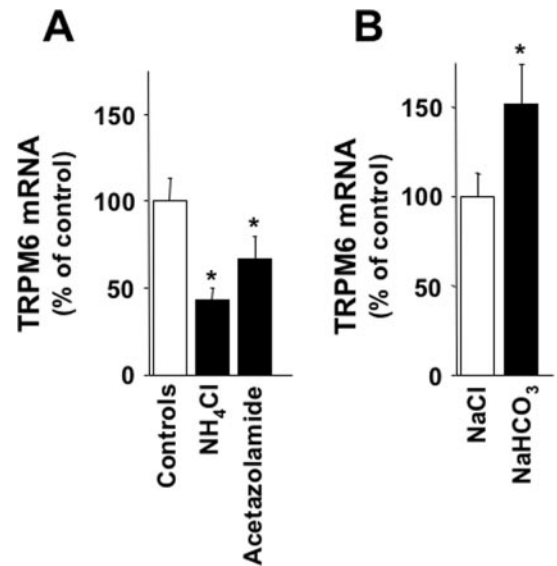


Figure 6. Effect of chronic metabolic acidosis and alkalosis on renal mRNA expression of the epithelial Mg²⁺ channel TRPM6 in wild-type mice. Renal mRNA expression levels of TRPM6 was determined during chronic metabolic acidosis and acetazolamide treatment (A) as well as chronic metabolic alkalosis (B) by real-time quantitative PCR analysis as the ratio of HPRT and depicted as percentage of respective controls. Controls, animals that received deionized drinking water only; NH₄Cl, animals that received 0.28 M NH₄Cl *via* the drinking water; Acetazolamide, animals that received acetazolamide (20 mg/kg per d) subcutaneously by osmotic minipump; NaCl, animals that received 0.2 M NaCl *via* the drinking water; NaHCO₃, animals that received 0.2 M NaHCO₃ *via* the drinking water; *n* = 9 animals per treatment group. Data are presented as means ± SEM. **P* < 0.05 *versus* respective control group (controls or NaCl-treated animals).

ing effect and increased renal expression of the Ca²⁺ transport proteins in wild-type mice. This suggests that the increased expression of these transporters is responsible for the hypocalciuric effect. However, TRPV5 ablation resulting in the functional lack of active Ca²⁺ transport did not preclude this effect, suggesting that upregulation of Ca²⁺ transport proteins in DCT/CNT is not crucial for the induction of hypercalciuria. It is interesting that alkalosis did not enhance calbindin-D_{28K} abundance in TRPV5^{-/-} mice. This is in line with previous studies from our laboratory, which demonstrated that blockade of the TRPV5-mediated Ca²⁺ influx in rabbit CNT/CCD cells downregulates calbindin-D_{28K} expression (39). This indicated that regulation of the latter protein is highly dependent on the presence of TRPV5. The bulk of filtered Ca²⁺ is reabsorbed by a passive paracellular mechanism that is localized primarily in the proximal tubule and to a lesser extent in TAL (1). In these nephron segments, Ca²⁺ reabsorption is secondary to Na⁺ reabsorption and the resulting water reabsorption, which creates a favorable electrochemical gradient driving passive Ca²⁺ transport. Determination of Li⁺ clearance indeed suggested that NaHCO₃-treated mice show increased proximal tubular Na⁺ reabsorption and, therefore, possibly display enhanced

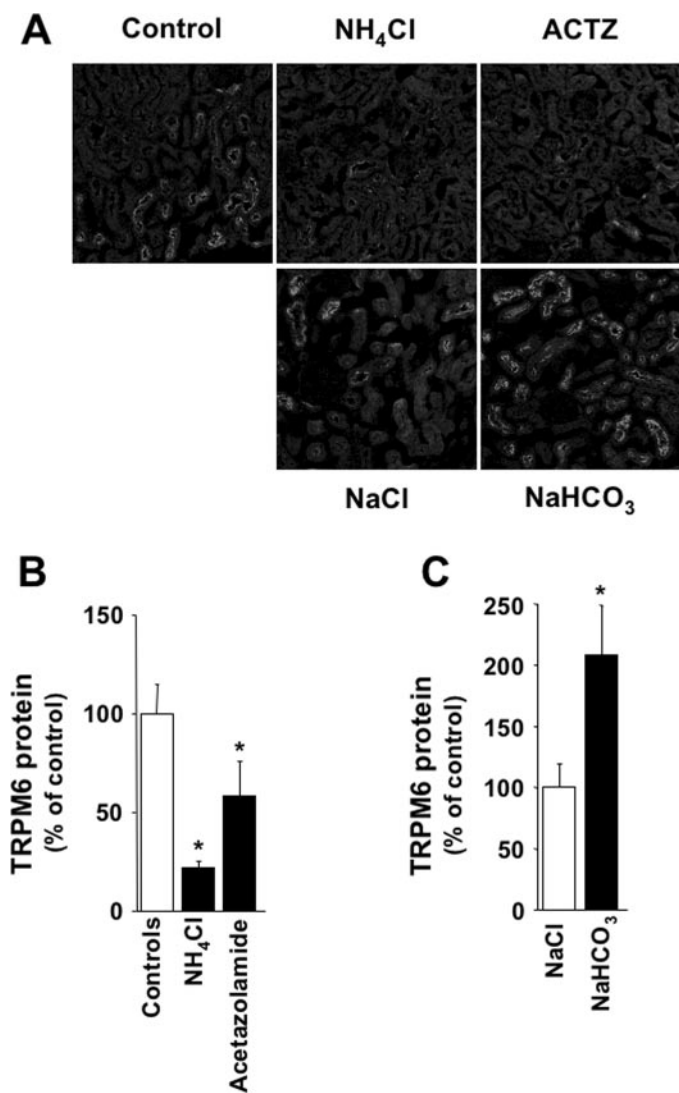


Figure 7. Effects of chronic metabolic acidosis and alkalosis on renal protein abundance of the epithelial Mg^{2+} channel TRPM6 in wild-type mice. Representative immunohistochemical imaging of TRPM6 staining in kidney cortex (A), which enabled semiquantitative determination of renal TRPM6 protein abundance during chronic metabolic acidosis and acetazolamide treatment (B) as well as chronic metabolic alkalosis (C) by computerized analysis. Data were calculated as IOD (arbitrary units) and depicted as percentage of respective controls. Controls, animals that received deionized drinking water only; NH_4Cl , animals that received 0.28 M NH_4Cl *via* the drinking water; ACTZ/Acetazolamide, animals that received acetazolamide (20 mg/kg per d) subcutaneously by osmotic minipump; NaCl, animals that received 0.2 M NaCl *via* the drinking water; $NaHCO_3$, animals that received 0.2 M $NaHCO_3$ *via* the drinking water; $n = 9$ animals per treatment group. Data are presented as means \pm SEM. * $P < 0.05$ *versus* respective control group (controls or NaCl-treated animals).

passive Ca^{2+} reabsorption compared with NaCl-treated controls. Thus, the hypocalciuria could alternatively be explained by increased passive Ca^{2+} reabsorption. Taken together, the present data offer insight into the previously unexplained

mechanism by which administration of HCO_3^- prevents nephrolithiasis in patients with recurrent kidney stones (40,41). Up-regulation of Ca^{2+} transport proteins in DCT/CNT occurs but is not crucial for the Ca^{2+} -sparing effect.

The epithelial Mg^{2+} channel TRPM6 is the first identified protein involved in active Mg^{2+} reabsorption (7–9). TRPM6 was localized along the apical membrane of DCT, and mutations in the gene encoding TRPM6 were shown to cause autosomal recessive hypomagnesemia, characterized by inappropriately high Mg^{2+} excretion and disturbed intestinal Mg^{2+} absorption. In our study, NH_4Cl -induced chronic metabolic acidosis decreased renal TRPM6 abundance accompanied by increased Mg^{2+} excretion and hypomagnesemia. Conversely, chronic metabolic alkalosis increased TRPM6 expression as well as renal Mg^{2+} reabsorption, resulting in hypermagnesemia. There is insufficient functional information available regarding the tubular segments that are involved in the altered Mg^{2+} reabsorption, but Wong *et al.* (10,42) previously demonstrated altered Mg^{2+} reabsorption in the distal tubule during metabolic acidosis and alkalosis in the dog. Furthermore, a high extracellular pH was shown to enhance Mg^{2+} uptake in isolated mouse DCT cells, and conversely a low pH diminished this uptake (43). Thus, these data suggest that alterations of acid-base status regulate TRPM6 expression, thereby affecting renal active Mg^{2+} reabsorption in DCT and leading to significant changes in serum Mg^{2+} . We previously demonstrated that thiazide administration as well as treatment with the hypomagnesemic immunosuppressant tacrolimus (FK506) reduces renal TRPM6 abundance accompanied by increased urine Mg^{2+} loss (15,16). Therefore, TRPM6 downregulation seems to be a general mechanism explaining the renal Mg^{2+} leak and resulting hypomagnesemia in these important clinical situations.

It is interesting that we showed that acetazolamide displays a Mg^{2+} -sparing effect in mice. This carbonic anhydrase inhibitor is also known to result in hypomagnesuria in human *via* an unknown mechanism (21–23). Importantly, TRPM6 expression was significantly diminished during chronic acetazolamide treatment. This suggests that chronic metabolic acidosis, irrespective of cause or associated urine pH, downregulates TRPM6 expression. At the same time, these data are against enhanced active Mg^{2+} reabsorption explaining the decreased Mg^{2+} excretion. In contrast to Ca^{2+} , the bulk of filtered Mg^{2+} is reabsorbed in TAL, where the $Na^+-K^+(NH_4^+)-2Cl^-$ (NKCC2) cotransporter is responsible for maintaining the required electrochemical gradient (44). Acetazolamide treatment was associated with increased urine volume and Na^+ excretion, which has been shown to result in extracellular volume contraction and enhanced NKCC2 activity (45,46). Furthermore, metabolic acidosis, which developed in acetazolamide-treated wild-type mice, was previously shown to increase NKCC2 mRNA and protein abundance (14,47). Thus, we postulate that these additive stimulatory effects enhance passive Mg^{2+} reabsorption in TAL. Alternatively, regulation of the tight junction protein paracellin-1, which is supposed to facilitate paracellular reabsorption of Mg^{2+} in TAL, might be involved (48,49). Together, these mechanisms could counteract the metabolic aci-

dosis-induced TRPM6 downregulation and result in a net Mg²⁺-sparing effect.

The mechanism translating the acid-base status to regulation of gene expression remains largely unknown. Our results show that transcriptional regulation occurs irrespective of urine pH. Because intracellular pH will ultimately reflect pH of the urine, apical or intracellular acid sensing does not seem to be involved. Therefore, direct sensing of acid-base status by pH-sensitive proteins at the basolateral membrane is likely. In DCT/CNT, the extracellular Ca²⁺/Mg²⁺-sensing receptor is expressed at the basolateral membrane (50,51). It was shown recently that extracellular pH directly influences the sensitivity of this receptor to Ca²⁺ and Mg²⁺ (52,53). Therefore, altered Ca²⁺/Mg²⁺ sensing might influence transcellular divalent transport in these nephron segments. Furthermore, other basolateral proton-sensing receptors or channels might act as an acid sensor regulating Ca²⁺ and Mg²⁺ transport protein expression (54,55). Thus, whereas the presented data demonstrated the transcriptional and translational regulation of proteins that are involved in active Ca²⁺ and Mg²⁺ reabsorption, future studies will have to elucidate the exact mechanism by which acid-base status affects expression of these transporters.

Acknowledgments

This work was financially supported by the Dutch Kidney Foundation (C10.1881, C03.6017) and the Dutch Organization of Scientific Research (Zon-Mw 016.006.001).

We thank the Central Animal Facility, Radboud University Nijmegen, for technical support.

References

- Hoenderop JG, Nilius B, Bindels RJ: Calcium absorption across epithelia. *Physiol Rev* 85: 373–422, 2005
- Sutton RA, Wong NL, Dirks JH: Effects of metabolic acidosis and alkalosis on sodium and calcium transport in the dog kidney. *Kidney Int* 15: 520–533, 1979
- Dai LJ, Ritchie G, Kerstan D, Kang HS, Cole DE, Quamme GA: Magnesium transport in the renal distal convoluted tubule. *Physiol Rev* 81: 51–84, 2001
- Lemann J Jr, Bushinsky DA, Hamm LL: Bone buffering of acid and base in humans. *Am J Physiol Renal Physiol* 285: F811–F832, 2003
- Hoenderop JG, Willems PH, Bindels RJ: Toward a comprehensive molecular model of active calcium reabsorption. *Am J Physiol Renal Physiol* 278: F352–F360, 2000
- Hoenderop JG, van der Kemp AW, Hartog A, van de Graaf SF, van Os CH, Willems PH, Bindels RJ: Molecular identification of the apical Ca²⁺ channel in 1,25-dihydroxyvitamin D₃-responsive epithelia. *J Biol Chem* 274: 8375–8378, 1999
- Voets T, Nilius B, van der Kemp AW, Droogmans G, Bindels RJ, Hoenderop JG: TRPM6 forms the Mg²⁺ influx channel involved in Mg²⁺ reabsorption. *J Biol Chem* 279: 19–25, 2004
- Schlingmann KP, Weber S, Peters M, Niemann Nejsum L, Vitzthum H, Klingel K, Kratz M, Haddad E, Ristoff E, Dinour D, Syrrou M, Nielsen S, Sassen M, Waldegger S, Seyberth HW, Konrad M: Hypomagnesemia with secondary hypocalcemia is caused by mutations in TRPM6, a new member of the TRPM gene family. *Nat Genet* 31: 166–170, 2002
- Walder RY, Landau D, Meyer P, Shalev H, Tsoia M, Bo-rochowitz Z, Boettger MB, Beck GE, Englehardt RK, Carmi R, Sheffield VC: Mutation of TRPM6 causes familial hypomagnesemia with secondary hypocalcemia. *Nat Genet* 31: 171–174, 2002
- Wong NL, Quamme GA, Dirks JH: Effects of acid-base disturbances on renal handling of magnesium in the dog. *Clin Sci (Lond)* 70: 277–284, 1986
- Amlal H, Sheriff S, Soleimani M: Upregulation of collecting duct aquaporin-2 by metabolic acidosis: Role of vasopressin. *Am J Physiol Cell Physiol* 286: C1019–C1030, 2004
- Wagner CA, Finberg KE, Stehberger PA, Lifton RP, Giebisch GH, Aronson PS, Geibel JP: Regulation of the expression of the Cl⁻/anion exchanger pendrin in mouse kidney by acid-base status. *Kidney Int* 62: 2109–2117, 2002
- Frische S, Kwon TH, Frokiaer J, Madsen KM, Nielsen S: Regulated expression of pendrin in rat kidney in response to chronic NH₄Cl or NaHCO₃ loading. *Am J Physiol Renal Physiol* 284: F584–F593, 2003
- Attmane-Elakeb A, Mount DB, Sibella V, Vernimmen C, Hebert SC, Bichara M: Stimulation by in vivo and in vitro metabolic acidosis of expression of rBSC-1, the Na⁺-K⁺(NH₄⁺)-2Cl⁻ cotransporter of the rat medullary thick ascending limb. *J Biol Chem* 273: 33681–33691, 1998
- Nijenhuis T, Hoenderop JG, Bindels RJ: Down-regulation of Ca²⁺ and Mg²⁺ transport proteins in the kidney explains tacrolimus (FK506)-induced hypercalciuria and hypomagnesemia. *J Am Soc Nephrol* 15: 549–557, 2004
- Nijenhuis T, Vallon V, van der Kemp AW, Loffing J, Hoenderop JG, Bindels RJ: Enhanced passive Ca²⁺ reabsorption and reduced Mg²⁺ channel abundance explains thiazide-induced hypocalciuria and hypomagnesemia. *J Clin Invest* 115: 1651–1658, 2005
- Hoenderop JG, van Leeuwen JP, van der Eerden B, Kersten F, van der Kemp AW, Merrliat A, Waarsing E, Rossier B, Vallon V, Hummler E, Bindels RJ: Renal Ca²⁺ wasting, hyperabsorption and reduced bone thickness in mice lacking TRPV5. *J Clin Invest* 112: 1906–1914, 2003
- Soleimani M: Na⁺:HCO₃⁻ cotransporters (NBC): Expression and regulation in the kidney. *J Nephrol* 15[Suppl 5]: S32–S40, 2002
- Soleimani M, Aronson PS: Effects of acetazolamide on Na⁺-HCO₃⁻ cotransport in basolateral membrane vesicles isolated from rabbit renal cortex. *J Clin Invest* 83: 945–951, 1989
- Dirks JH, Cirksena WJ, Berliner RW: Micropuncture study of the effect of various diuretics on sodium reabsorption by the proximal tubules of the dog. *J Clin Invest* 45: 1875–1885, 1966
- Sutton RA, Walker VR: Responses to hydrochlorothiazide and acetazolamide in patients with calcium stones. Evidence suggesting a defect in renal tubular function. *N Engl J Med* 302: 709–713, 1980
- Durlach J: *Magnesium in Clinical Practice*, London, John Libbey, 1988
- Itokawa Y, Durlach J: *Magnesium in Health and Disease (Fifth International Magnesium Symposium)*, Kyoto, Japan, London, John Libbey, 1989
- Stauber A, Radanovic T, Stange G, Murer H, Wagner CA, Biber J: Regulation of intestinal phosphate transport. II.

- Metabolic acidosis stimulates Na⁺-dependent phosphate absorption and expression of the Na⁺-Pi cotransporter NaPi-IIb in small intestine. *Am J Physiol Gastrointest Liver Physiol* 288: G501–G506, 2005
25. Hoenderop JG, Muller D, Van Der Kemp AW, Hartog A, Suzuki M, Ishibashi K, Imai M, Sweep F, Willems PH, Van Os CH, Bindels RJ: Calcitriol controls the epithelial calcium channel in kidney. *J Am Soc Nephrol* 12: 1342–1349, 2001
 26. van Abel M, Hoenderop JG, Dardenne O, St-Arnaud R, Van Os C, van Leeuwen JP, Bindels RJ: 1,25(OH)₂D₃-independent stimulatory effect of estrogen on the expression of ECaC1 in kidney. *J Am Soc Nephrol* 13: 2102–2109, 2002
 27. Nijenhuis T, Hoenderop JG, Loffing J, van der Kemp AW, Van Os C, Bindels RJ: Thiazide-induced hypocalciuria is accompanied by a decreased expression of Ca²⁺ transporting proteins in the distal tubule. *Kidney Int* 64: 555–564, 2003
 28. Hoenderop JG, Hartog A, Stuiver M, Doucet A, Willems PH, Bindels RJ: Localization of the epithelial Ca²⁺ channel in rabbit kidney and intestine. *J Am Soc Nephrol* 11: 1171–1178, 2000
 29. Krieger NS, Frick KK, Bushinsky DA: Mechanism of acid-induced bone resorption. *Curr Opin Nephrol Hypertens* 13: 423–436, 2004
 30. Rizzo M, Capasso G, Bleich M, Pica A, Grimaldi D, Bindels RJ, Greger R: Effect of chronic metabolic acidosis on calbindin expression along the rat distal tubule. *J Am Soc Nephrol* 11: 203–210, 2000
 31. Vennekens R, Prenen J, Hoenderop JG, Bindels RJ, Droogmans G, Nilius B: Modulation of the epithelial Ca²⁺ channel ECaC by extracellular pH. *Pflugers Arch* 442: 237–242, 2001
 32. Yeh BI, Sun TJ, Lee JZ, Chen HH, Huang CL: Mechanism and molecular determinant for regulation of rabbit transient receptor potential type 5 (TRPV5) channel by extracellular pH. *J Biol Chem* 278: 51044–51052, 2003
 33. Preisig PA, Alpern RJ: Chronic metabolic acidosis causes an adaptation in the apical membrane Na/H antiporter and basolateral membrane Na(HCO₃) symporter in the rat proximal convoluted tubule. *J Clin Invest* 82: 1445–1453, 1988
 34. Ambuhl PM, Amemiya M, Danczkay M, Lotscher M, Kaissling B, Moe OW, Preisig PA, Alpern RJ: Chronic metabolic acidosis increases NHE3 protein abundance in rat kidney. *Am J Physiol* 271: F917–F925, 1996
 35. Wu MS, Biemesderfer D, Giebisch G, Aronson PS: Role of NHE3 in mediating renal brush border Na⁺-H⁺ exchange. Adaptation to metabolic acidosis. *J Biol Chem* 271: 32749–32752, 1996
 36. Laghmani K, Preisig PA, Moe OW, Yanagisawa M, Alpern RJ: Endothelin-1/endothelin-B receptor-mediated increases in NHE3 activity in chronic metabolic acidosis. *J Clin Invest* 107: 1563–1569, 2001
 37. Tawil R, Moxley RT 3rd, Griggs RC: Acetazolamide-induced nephrolithiasis: Implications for treatment of neuromuscular disorders. *Neurology* 43: 1105–1106, 1993
 38. Ahlstrand C, Tiselius HG: Urine composition and stone formation during treatment with acetazolamide. *Scand J Urol Nephrol* 21: 225–228, 1987
 39. van Abel M, Hoenderop JG, Friedlaender MM, van Leeuwen JP, Bindels RJ: Coordinated regulation of renal calcium transport proteins by parathyroid hormone. *Kidney Int* 68: 1708–1721, 2004
 40. Lemann J Jr, Gray RW, Pleuss JA: Potassium bicarbonate, but not sodium bicarbonate, reduces urinary calcium excretion and improves calcium balance in healthy men. *Kidney Int* 35: 688–695, 1989
 41. Preminger GM, Sakhaee K, Pak CY: Alkali action on the urinary crystallization of calcium salts: Contrasting responses to sodium citrate and potassium citrate. *J Urol* 139: 240–242, 1988
 42. Shapiro RJ, Yong CK, Quamme GA: Influence of chronic dietary acid on renal tubular handling of magnesium. *Pflugers Arch* 409: 492–498, 1987
 43. Dai LJ, Friedman PA, Quamme GA: Acid-base changes alter Mg²⁺ uptake in mouse distal convoluted tubule cells. *Am J Physiol* 272: F759–F766, 1997
 44. Quamme GA, de Rouffignac C: Epithelial magnesium transport and regulation by the kidney. *Front Biosci* 5: D694–D711, 2000
 45. Kwon TH, Nielsen J, Kim YH, Knepper MA, Frokiaer J, Nielsen S: Regulation of sodium transporters in the thick ascending limb of rat kidney: Response to angiotensin II. *Am J Physiol Renal Physiol* 285: F152–F165, 2003
 46. Knepper MA, Brooks HL: Regulation of the sodium transporters NHE3, NKCC2 and NCC in the kidney. *Curr Opin Nephrol Hypertens* 10: 655–659, 2001
 47. Karim Z, Attmane-Elakeb A, Sibella V, Bichara M: Acid pH increases the stability of BSC1/NKCC2 mRNA in the medullary thick ascending limb. *J Am Soc Nephrol* 14: 2229–2236, 2003
 48. Simon DB, Lu Y, Choate KA, Velazquez H, Al-Sabban E, Praga M, Casari G, Bettinelli A, Colussi G, Rodriguez-Soriano J, McCredie D, Milford D, Sanjad S, Lifton RP: Paracellin-1, a renal tight junction protein required for paracellular Mg²⁺ resorption. *Science* 285: 103–106, 1999
 49. Blanchard A, Jeunemaitre X, Coudol P, Dechaux M, Froissart M, May A, Demontis R, Fournier A, Paillard M, Houillier P: Paracellin-1 is critical for magnesium and calcium reabsorption in the human thick ascending limb of Henle. *Kidney Int* 59: 2206–2215, 2001
 50. Riccardi D, Park J, Lee WS, Gamba G, Brown EM, Hebert SC: Cloning and functional expression of a rat kidney extracellular calcium/polyvalent cation-sensing receptor. *Proc Natl Acad Sci U S A* 92: 131–135, 1995
 51. Riccardi D, Hall AE, Chattopadhyay N, Xu JZ, Brown EM, Hebert SC: Localization of the extracellular Ca²⁺/polyvalent cation-sensing protein in rat kidney. *Am J Physiol* 274: F611–F622, 1998
 52. Quinn SJ, Bai M, Brown EM: pH sensing by the calcium-sensing receptor. *J Biol Chem* 279: 37241–37249, 2004
 53. Doroszewicz J, Waldegger P, Jeck N, Seyberth H, Waldegger S: pH dependence of extracellular calcium sensing receptor activity determined by a novel technique. *Kidney Int* 67: 187–192, 2005
 54. Gluck SL: Acid sensing in renal epithelial cells. *J Clin Invest* 114: 1696–1699, 2004
 55. Ludwig MG, Vanek M, Guerini D, Gasser JA, Jones CE, Junker U, Hofstetter H, Wolf RM, Seuwen K: Proton-sensing G-protein-coupled receptors. *Nature* 425: 93–98, 2003